Structural Engineering and Mechanics, Vol. 41, No. 6 (2012) 711-734
DOI: http://dx.doi.org/10.12989/sem.2012.41.6.711

Nonlinear interaction behaviour of plane frame-layered soil system subjected to seismic loading

Ramakant Agrawal*[1] and M.S. Hora[2]

[1]*Department of Civil Engineering,TRUBA Institute of Engineering and Information Technology, Bhopal, India*
[2]*Department of Applied Mechanics, Maulana Azad National Institute of Technology, Bhopal, India*

(Received November 10, 2010, Revised February 12, 2012, Accepted February 21, 2012)

Abstract. The foundation of a tall building frame resting on settable soil mass undergoes differential settlements which alter the forces in the structural members significantly. For tall buildings it is essential to consider seismic forces in analysis. The building frame, foundation and soil mass are considered to act as single integral compatible structural unit. The stress-strain characteristics of the supporting soil play a vital role in the interaction analysis. The resulting differential settlements of the soil mass are responsible for the redistribution of forces in the superstructure. In the present work, the nonlinear interaction analysis of a two-bay ten-storey plane building frame- layered soil system under seismic loading has been carried out using the coupled finite-infinite elements. The frame has been considered to act in linear elastic manner while the soil mass to act as nonlinear elastic manner. The subsoil in reality exists in layered formation and consists of various soil layers having different properties. Each individual soil layer in reality can be considered to behave in nonlinear manner. The nonlinear layered system as a whole will undergo differential settlements. Thus, it becomes essential to study the structural behaviour of a structure resting on such nonlinear composite layered soil system. The nonlinear constitutive hyperbolic soil model available in the literature is adopted to model the nonlinear behaviour of the soil mass. The structural behaviour of the interaction system is investigated as the shear forces and bending moments in superstructure get significantly altered due to differential settlements of the soil mass.

Keywords: conventional frame analysis; finite element method; plane frame; soil-structure interaction; nonlinear analysis; hyperbolic soil model; differential settlement; decay pattern; infinite elements; truncation boundary

1. Introduction

In common structural design practice the foundation loads from structural analysis are obtained without considering allowance for soil settlements. The foundation settlements are estimated assuming a perfectly flexible structure. Such an analysis of frame-foundation-soil system may often lead to unrealistic solution and sometimes, it may lead to failure as the stiffness of the structure can restrain the displacements of the foundations and even small differential settlements of the foundations may also alter the forces of the structural members significantly. It is necessary to consider building frame, foundation and soil as single integral compatible structural unit for realistic analysis.

*Corresponding author, Ph.D. Student, E-mail: rk_agrawal006@rediffmail.com

In reality, the stress-strain response of soil mass is nonlinear and needs a numerical technique to model its behaviour. The finite element method is a powerful numerical tool for numerical analysis of any soil-structure interaction problem. Before the development of infinite elements, the conventional finite element method was used to model the unbounded domain of soil mass extending to infinity in one or two direction. The finite element mesh was truncated at some large but finite distance. This type of approximation to infinity proved to be uneconomical and expensive. The coupled finite-infinite isoparametric elements are numerically very powerful and computationally economical to model the far field behaviour of the unbounded domain of the soil mass with proper location of truncation boundary (the common junction between the finite and infinite elements). The infinite element with exponential decay pattern is adopted to model the far field behaviour of the soil mass.

In the present analysis, the interaction behaviour of plane frame-layered soil mass with respect to differential settlement is studied.

2. Literature review

Numerous studies e.g., Meyarhoff (1947), Francis (1953), Chameski (1956), Greshoff (1957), Baker (1957), Morries (1966), Larnach (1970), Lee and Brown (1972), Seetharamulu and Kumar (1973), King and Chandrasekaran (1974), Jain *et al*. (1977), Salvadurai (1989), King and Yao (1983), Subbarao (1985), Nayak *et al*. (1972), Brown and Yu (1986), Sharda Bai *et al*. (1990), Allam *et al*. (1991), Viladkar and Godbole (1991), McCallen *et al.* (1993), Dutta and Bhattacharya (1999), Kim and Yun (2003) and Hora and Patel (2005) have made to quantify the effect of soil-structure interaction on building frames. These studies have clearly indicated that force quantities are revised due to interaction phenomenon.

Aljanabi *et al*. (1990) studied the interaction of plane frames with an elastic foundation of the Winkler's type, having normal and shear moduli of sub-grade reactions. An exact stiffness matrix for a beam element on an elastic foundation having only a normal modulus of sub-grade reaction was modified to include the shear modulus of sub-grade reaction of the foundation as well as the axial force in the beam. The results indicated that bending moments might be considerably affected according to the type of frame and loading.

Viladkar *et al*. (1991) used coupled finite-infinite elements for modeling of superstructure-soil mass interaction and considered the soil mass to behave nonlinearly. It provided the best means of idealizing a soil-structure interaction problem. The research work is noteworthy in the sense that it provided great improvement over physical modelling of the problem and the far-field domain (soil) was best modeled by infinite elements with different types of decay. This saves lot of computational efforts and is cost effective. The approach is very attractive, logical, more rational and easy for computer implementation. In the present research work, this approach will be worth adopting.

Noorzaei *et al*. (1994) presented the influence of strain hardening on soil-structure interaction analysis of a plane frame-combined footing-soil system taking into account the elasto-plastic behaviour of the compressible sub-soil and its strain hardening characteristics.

Fardis and Panagiostakos (1997) studied the effects of masonry infills on the global seismic response of reinforced concrete structure by numerical analysis. In this study, response spectra of elastic SDOF frames with nonlinear infills show that despite their apparent stiffening effect on the system infills reduce spectral displacements and forces mainly through their high damping in the

first large post-cracking excursion. The study concludes that due to the hysteretic is reduced, without an increase in the seismic force demands. They also found that the effects of soft-ground storey are not so important for seismic motion at the design intensity, but may be very large at higher motion intensities.

Mandal *et al*. (1998) proposed a computational iterative scheme for studying the effect of soil-structure interaction on axial force, column moment and finally adjusted foundation settlement of building frame. The results obtained from this computational scheme were validated from experimental study. They analyzed a small-scale two-storeyed two-bay frame made of Perspex. The frame is placed on a kaolin bed with adequate arrangement of drainage. The proposed computational scheme could be used to predict increase in axial force and moments in structural members due to the effect of soil- structure interaction

Manos *et al*. (2000) studied the influence of masonry infill on the earthquake response of multi-storey reinforced concrete structure. In this study, two test sequences were presented: first a 7-storey 2-D plane frame model on 1/12.5 scale, was tested at the Earthquake Simulator of Aristotale University whereas the second, a much larger model, of a 6-storey frame, on 1/3 scaled, (3-D frame) model located at the European Test Site at Volfi. Both structures were examined with and without masonry infill.

Kim and Yun (2003) presented time domain method for soil-structure interaction analysis under seismic excitation. It is based on the finite element formulation incorporating infinite elements for the far field soil region. Equivalent earthquake input forces are calculated based on the far-field soil regions utilizing the fixed exterior boundary method in the frequency domain. Earthquake response analyses were carried out on a multi-layered half-space and tunnel embedded in a layered half space with the assumption of the linearity of the near and far field soil region and results are compared with those obtained by the conventional method in the frequency domain.

Asteris (2003) investigated the influence of the masonry infill panel opening in the reduction of the infilled frames stiffness. A parametric study has been carried out using as parameters the position and the percentage of the masonry infill panel opening for the case of one-story one-bay infilled frame. The investigation has been extended to the case of multistory, fully or partially infilled frames. In particular, the redistribution of action effects of infilled frames under lateral loads has been studied. It is shown that the redistribution of shear force is critically influenced by the presence and continuity of infill panels. The presence of infills leads, in general, to decreased shear forces on the frame columns. However, in the case of an infilled frame with a soft ground story, the shear forces acting on columns are considerably higher than those obtained from the analysis of the bare frame.

Hora and Patel (2005) proposed computational methodology for non-linear soil-structure interaction analysis of infilled building frames. Underscoring the necessity of proper physical modeling of infilled building frame-foundation beam soil mass to assess more realistic and accurate structural behaviour, they discretized the unbounded domain of the soil mass with coupled finite-infinite elements to achieve the computational economy. The non-linear hyperbolic model was adopted to account for the non-linear stress-strain behaviour of the soil mass. The results revealed the significance of the non-linearity of soil mass in the response of the structure.

Hora (2006) further extended the work and revealed that apart from non-linearity of soil mass, inclusion of infill walls in the frame causes the redistribution of forces in the members of frame.

Kaushik *et al*. (2006) reviewed and compared analysis and design provisions related to MI-RC frames (Masonry infill-reinforced concrete frames), in seismic design codes of 16 countries and

identifies important issues that should be addressed by a typical model code.

Abate *et al*. (2007) investigated the dynamic seismic response of a fire station building structure considering soil plasticity and soil-foundation plastic hinges. The sliding at the soil foundation interface, uplifting of the foundation from the soil and mobilization of bearing capacity failure have been taken into account. He also investigated the effects of soil elasto-plastic constitution equation and foundation uplifting on the acceleration transmission and so on the structures bending moments and shear forces.

Asteris (2008) proposed a realistic criterion to describe the frame-infill separation in order to better simulate the complicated behavior of infilled frames under lateral loads. The basic characteristic of the analysis was that the contact lengths between the infill and the contact stresses are estimated as an integral part of the solution. Using this analysis, the response of a single-bay single storey masonry infilled RC frame, under a lateral load at the beam level, was investigated. The large magnitude of the variation of the contact lengths between the infill and the different frame members were presented.

Mohebkhah *et al*. (2008) proposed a two-dimensional numerical model using the specialized discrete element method (DEM) software UDEC (2004) developed for the nonlinear static analysis of masonry-infilled steel frames with openings subjected to in-plane monotonic loading. In this model, large displacements and rotations between masonry blocks are taken into account. It was found that the model can be used confidently to predict collapse load, joint cracking patterns and explore the possible failure modes of masonry-infilled steel frames with a given location for openings and relative area. Results from the numerical modeling and previous experimental studies found in the literature are compared which indicate a good correlation between them. Furthermore, a nonlinear analysis was performed to investigate the effect of door frame on lateral load capacity and stiffness of infilled frames with a central opening.

Monica *et al.* (2009) proposed a model to investigate the behaviour of infill panels in framed structures. The proposed model is based on the equivalent strut model, the concept of a plastic concentrator and damage mechanism. First some fundamental concepts of damage mechanism was briefly presented. Then, an experimental study of the behaviour of masonry specimens under compression forces was described. These results were used for the development of the constitutive law for the equivalent strut bars. The model was analyzed, first in the case of monotonic loadings, and then for cyclic loadings. Finally, the model was validated by numerical simulation of a test carried out on infilled frames subjected to monotonic and cyclic loadings

In the present study, the nonlinear stress-strain characteristic of the soil mass is modeled with well known hyperbolic model (Kondner and Zelasko 1963). The effect of differential settlements on the forces in the frame members and the contact pressure distribution below the footings is investigated. The seismic forces have been evaluated by static method as per Bureau of Indian Standard. The building frame is assumed to be located in most severe earthquake zone V.

3. Coupled finite-infinite elements modeling of interaction system

The idealization of plane frame-foundation-soil interaction system is achieved with isoparametric finite and infinite elements. The floor beams, the columns and the plinth beam are discretized using three node beam bending elements with three degrees of freedom per node (u, v, θ). The unbounded domain of the soil mass is represented by eight node conventional plane strain finite elements

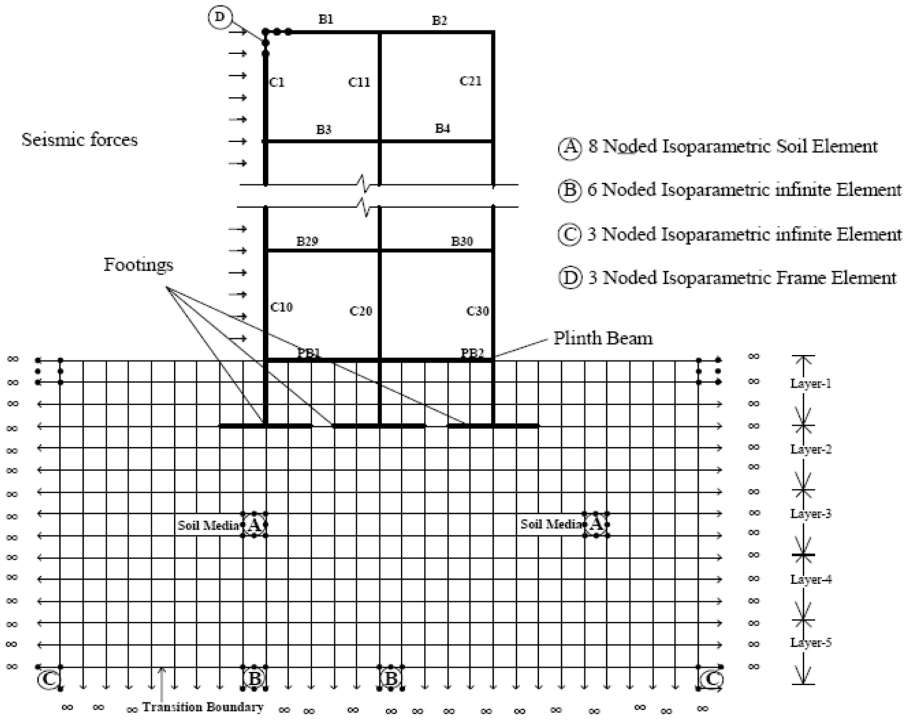

Fig. 1 Finite-infinite element idealization of plane frame-layered soil system

coupled with six node infinite elements with exponential type decay with two degrees of freedom per node (u, v) (Viladkar *et al*. 1991). A doubly infinite element is used as corner element in the finite-infinite element mesh. Fig. 1 shows the discretization of the interaction system.

4. Nonlinear elastic hyperbolic soil model

In the present problem, there are mainly two types of materials involved: reinforced concrete and the soil. The stiffness of the reinforced concrete is much higher in comparison to that of soil. Therefore, in this study, material nonlinearity of the soil mass is considered while the reinforced concrete is assumed to follow the linear stress-strain relationship. The non-linearity of soil mass has been represented using the hyperbolic model proposed by Kondner (1963). The model is used in the literature by Duncan and Chang (1970) for nonlinear stress analysis of soil. The tangent modulus (E_T), of the soil mass at any deviatoric stress level is represented as

$$E_T = \left[1 - \frac{R_f(1-\sin\phi)(\sigma_1-\sigma_3)}{2(c\cos\phi+\sigma_3\sin\phi)}\right]^2 E_i \tag{1}$$

Where

$$E_i = KP_a\left(\frac{\sigma_3}{P_a}\right)^n \tag{2}$$

Table 1 Soil properties for nonlinear analysis

Description	Symbol	Numerical Values				
		Layer 1	Layer 2	Layer 3	Layer 4	Layer 5
Initial tangent modulus (kN/m^2)	E_i	35000	40000	50000	55000	60000
Poisson's ratio	μ	0.28	0.29	0.30	0.32	0.33
Cohesion (kN/m^2)	c	0.0	0.0	0.0	0.0	0.0
Angle of internal friction	Ø	37.5	37.6	37.65	37.7	37.76
Modulus number	K	500.0	501.0	501.5	501.8	502.0
Exponent	n	0.92	0.91	0.91	0.90	0.90
Failure ratio	R_f	0.85	0.84	0.83	0.83	0.82
Atmospheric pressure (kN/m^2)	P_a	100.00	100.0	100.00	100.00	100.00
Thickness of layer (m)	-	4.50	11.50	7.00	8.00	39.00

Various parameters representing the non-linearity of soil mass are:
E_i = Initial tangent modulus
c = Cohesion
P_a = Atmospheric pressure
σ_1, σ_3 = Major and the minor principal stresses
ϕ = Angle of internal friction
K = Modulus number
n = Exponent determining the variation of initial tangent modulus E_i, with confining pressure σ_3.

$$R_f = \text{Failure ratio} = \frac{(\sigma_1 - \sigma_3)_f}{(\sigma_1 - \sigma_3)_{ult}}$$

Where,
$(\sigma_1 - \sigma_3)_f$ = Compressive strength
$(\sigma_1 - \sigma_3)_{ult}$ = Asymptotic value of deviatoric stress
The values of these parameters taken in this study are indicated in Table 1. Poisson's ratio has been kept constant in the analysis. This hyperbolic model has been incorporated into the computer code developed for nonlinear analysis.

5. Computational algorithm

The mixed (incremental-iterative) technique has been adopted for the nonlinear elastic analysis of the present problem (Noorzaei 1991). The vertical load is applied in increments. The stiffness matrix of the soil mass is regenerated at the beginning of the first iteration of every load increment. The computational steps involved are provided here.

First Load Increment:

Let $\{\Delta P\}$ and $[K]$ denote the incremental force vector and the stiffness matrix of the system and $\{\Delta\delta\}$, $\{\Delta\varepsilon\}$ and $\{\Delta\sigma\}$ denote the incremental deformations, strains and stresses respectively.

(i) First iteration: Evaluate incremental deformations as

$$\{\Delta P\}_1^1 = [K]_1^1\{\Delta\delta\}_1^1 \tag{3}$$

(ii) Solve (Eq. 5.1) for {Dd} and evaluate the incremental strains and stresses as

$$\begin{aligned}\{\Delta\varepsilon\}_1^1 &= [B]\{\Delta\delta\}_1^1\\ \{\Delta\sigma\}_1^1 &= [D]_1^1\{\Delta\varepsilon\}_1^1\end{aligned} \tag{4}$$

$[B]$ and $[D]$ are strain-displacement and elasticity matrices respectively.

(iii) Accumulate the current incremental stresses and converged stresses upto previous iteration into temporary stresses as

$$\{\sigma\}_{1,temp}^1 = \{\sigma\}_{0,acc}^1 + \{\Delta\sigma\}_1^1 \tag{5}$$

Where $\{\sigma\}_{0,acc}^1$ is the accumulated stress and is initially zero at the beginning of first iteration of first load increment.

(iv) Evaluate principal stresses σ_1 and σ_3 using above temporary stresses.

(v) Evaluate tangent modulus of soil mass (E_T) for the current stress level using (Eq. (1)).

(vi) Modify [D] matrix on the basis of tangent modulus and evaluate modified stresses as

$$\{\Delta\sigma\}_{1,\mathrm{mod}}^1 = [D]_{1,\mathrm{mod}}^1\{\Delta\varepsilon\}_1^1 \tag{6}$$

(vii) Accumulate stresses as

$$\{\sigma\}_{1,acc}^1 = \{\sigma\}_{0,1cc}^1 + \{\Delta\sigma\}_{1,\mathrm{mod}}^1 \tag{7}$$

(viii) Evaluate residual force $\{Y\}$ as

$$\{\psi\}_1^1 = -\int[B]\{\sigma\}_{1,acc}^1 dV + \{\Delta P\}_1^1 \tag{8}$$

Solve the set of equations with these residual forces to achieve equilibrium.

(ix) Finally, accumulate the displacements

$$\{\delta\}_{1,acc}^1 = \{\delta\}_{0,acc}^1 + \{\Delta\delta\}_1^1 \tag{9}$$

(x) Check for convergence: In nonlinear analysis, the norm of displacements or norm of residual forces is selected for convergence. The present analysis considers the norm of residual forces. A tolerance limit of 3% is selected for the residual force. The maximum number of iterations for each load increment was fixed as 200 where the iterations must stop, if the solution does not converge. When the solution converges for a load increment, switch over to next load increment and repeat the steps (i) to (vii). For subsequent load increments, the stiffness matrix is modified on the basis of the stresses accumulated at the end of previous load increment and the above process is repeated till convergence takes place.

6. Nonlinear interaction analysis software

The computer programme has been developed in FORTRAN-90 for nonlinear interaction analysis

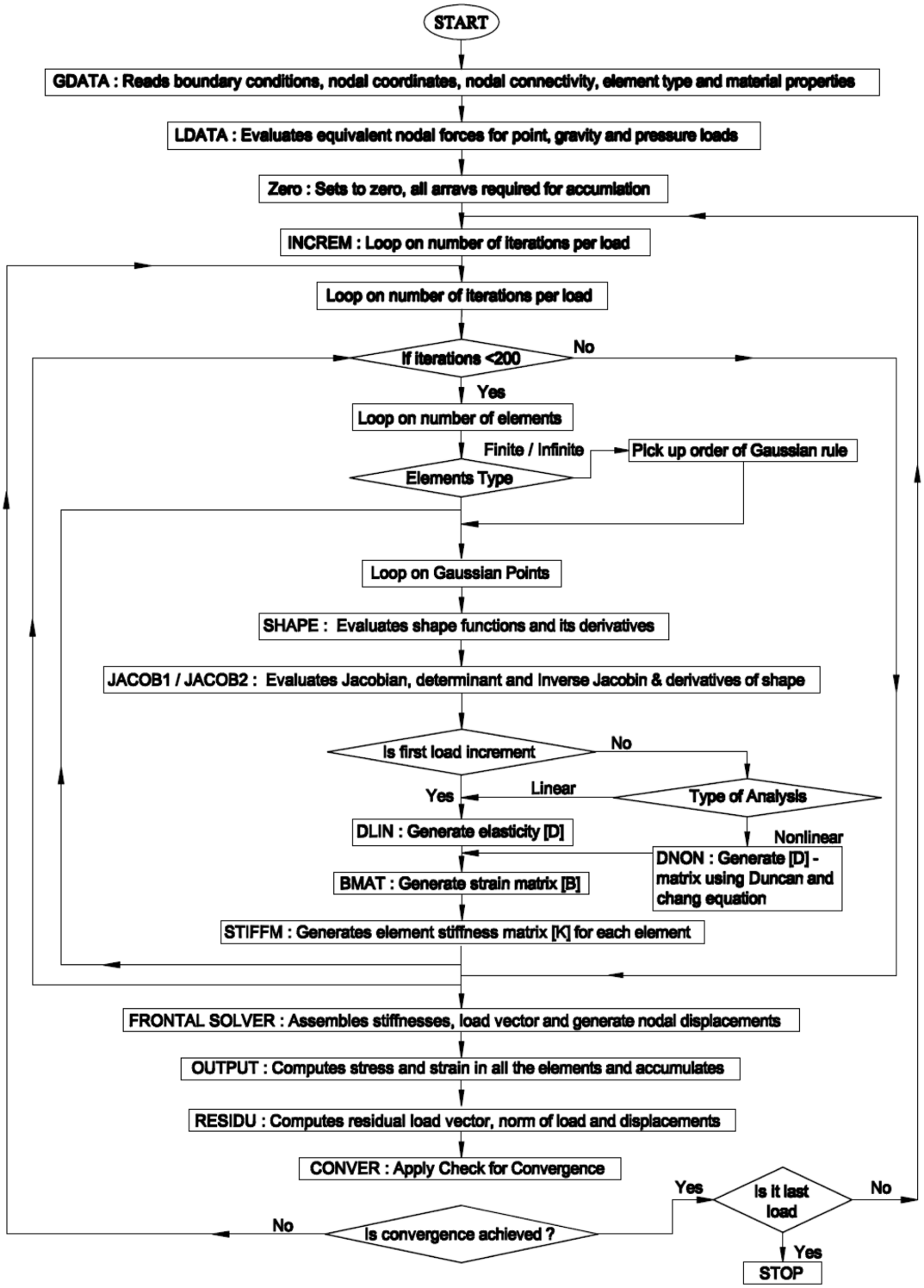

Fig. 2 Software for nonlinear elastic soil-structure interaction analysis

of frame-foundation beam-soil system. It includes a library of elements needed for the discretization of domain of the interaction system. The beam element included in the programme is the modified form of the beam-bending element (Hinton and Owen 1977), which includes one additional degree of freedom to take care of axial deformation in the frame members. The mixed incremental-iterative nonlinear algorithm is implemented in the programme to take care of nonlinear soil behaviour. The gauss-Legendre scheme is employed for the evaluation of element stiffness of finite and infinite elements both. In the present study, a frontal equation solver proposed by Godbole *et al*. (1991) is further modified and made compatible to the present problem. The flow chart for nonlinear interaction analysis is depicted in Fig. 2.

7. Interaction analysis

7.1 Location of truncation boundary

In any coupled finite-infinite element formulation, the most important aspect is the location of truncation boundary (the common junction between the finite and infinite element layer), which requires trial and error. To locate a truncation boundary, firstly 2-3 layers of finite elements are taken and one layer of infinite layer is attached below. Thereafter, each trial involves shifting its position by including an additional finite element layer above it. The deflection below any selected nodal point is compared with the result provided by fully finite element discretization of the problem to access the correct location of the truncation boundary.

In the present analysis, thirteen layers of finite elements were required which extended to a depth of nine times of the bay width whereas coupled analysis required only eleven layers of finite elements and one layer of infinite elements extending to depth of about four times the bay width. Moreover, the displacements of the free nodes of the infinite elements were found to be almost negligible which justifies the location of the truncation boundary. For location of truncation boundary, the behaviour of soil mass is treated as linear elastic.

7.2 Nonlinear analysis

In the present investigation, the linear elastic interaction analysis (LIA) and nonlinear interaction analysis (NLIA) of two-bay ten-storey plane frame- layered soil system has been carried out considering the frame to behave in linear elastic manner whereas the subsoil to behave in nonlinear elastic manner. The building frame has a bay width of 4.5 m and total height of 30.0 m. The floor beams and the plinth beam carry total uniformly distributed load of intensity 40 kN/m (dead load and live load). Table 2 shows geometrical and material properties of the superstructure

The seismic loads have been calculated by static method as per IS code IS1893 (Part I):2002 considering seismic zone V. The parameters used for estimation of the seismic forces are given in Table 3 and estimated seismic forces are provided in Table 4.

The nonlinear interaction analysis is carried out using mixed incremental-iterative algorithm. In the present analysis, the total vertical load of 3960 kN and seismic loads are applied in twelve load increments. Initially, the behaviour of the interaction system is linear elastic up to certain load value corresponding to the first load increment of 30% of the total load. Thereafter, the curve becomes nonlinear and, therefore, the remaining load increments are smaller (10, 10, 10, 5, 5, 5, 5, 5, 5, 5

Table 2 Geometrical and material properties of the superstructure

Sr. No	Structural components	Properties and size of component		
1	All floor and plinth beams	0.30 m × 0.40 m		
2	Columns	Floor	Outer	Inner
		I and II	0.30 m × 0.30 m	0.40 m × 0.40 m
		III and IV	0.35 m × 0.35 m	0.50 m × 0.50 m
		V and VI	0.40 m × 0.40 m	0.60 m × 0.60 m
		VII and VIII	0.50 m × 0.50 m	0.70 m × 0.70 m
		IX and X	0.60 m × 0.60 m	0.80 m × 0.80 m
3	Footings	3.0 m × 3.0 m × 1.0 m		
4	Number of bays	2		
5	Number of storeys	10		
6	Bay width	4.5		
7	Modulus of elasticity of concrete	2.1×10^7 kN/m^2		
8	Poisson's ratio of concrete	0.20		
9	Floor beam and plinth beam/ uniformly distributed loading	40 kN/m		

Table 3 Parameter used for estimation of seismic forces

Sr. No.	Parameter/Particulars	Value/type
1	Seismic zone	V
2	Seismic intensity	Severe
3	Zone factor	0.36
4	Type of soil	medium
5	Importance factor	1.0
6	Type of building	Moment resisting plane building frame
7	Response reduction factor	5.0

Table 4 Seismic forces at different floor levels

Floor level	I	II	III	IV	V	VI	VII	VIII	XI	X (Roof level)
Seismic force (kN)	0.6	2.5	5.5	9.7	15.0	21.4	28.8	37.2	46.6	37.8

and 5% of total load) as compared to initial elastic portion of the curve. The twelfth load increment corresponds to load factor 1.0 (i.e., total load on the structure). The norm of residual force for convergence is adopted and a tolerance limit of 3% is selected for residual forces.

The interaction behaviour is studied with respect to differential settlements caused due to incrementally applied loads of the nonlinear analysis. The variation of axial forces in the columns,

Table 5 Different types of elements for discretization

Sr. No.	Type of Element	Number of Elements
1	8 Noded panel element	480
2	8 Noded finite soil element	598
3	6 Noded infinite soil element	72
4	3 Noded doubly infinite soil element	2
5	3 Noded beam bending element	256
	Total number of elements	1429
	Total number of nodes	3580

bending moments in the columns, floor and plinth beams have been investigated due to increase in the differential settlements. The results of the nonlinear interaction analysis are compared with linear interaction analysis. The details of finite element discretization of the problem under investigation are depicted in Table 5.

7.2.1 Load versus differential settlement

In the present problem the differential settlement between left footing and middle footing (DS-LM) and between right and middle footing (DS-MR) is considered to investigate the structural behaviour of the plane frame-layered soil system. Fig. 3 depicts the variation of differential settlement with the load increments of nonlinear analysis (NLIA) of plane frame-layered soil system. The differential settlement between left and middle footings varies from 7.94 mm (first load increment) to 24.4 mm (twelfth load increment) and the variation is found to be bilinear. The value of differential settlement provided by LIA is found to be 19.95 mm.

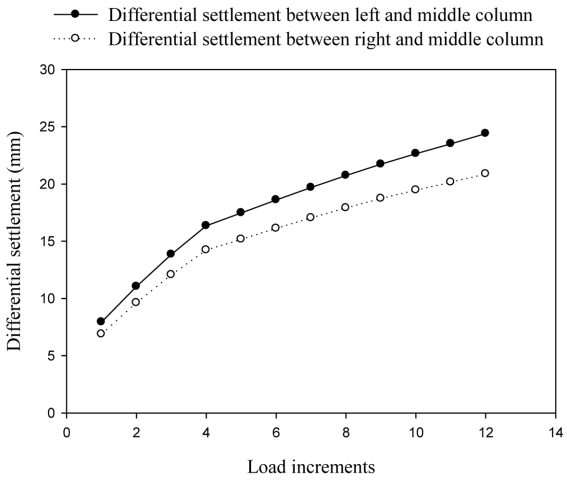

Fig. 3 Variation of differential settlement with load increments of nonlinear analysis of plane frame-layered soil system

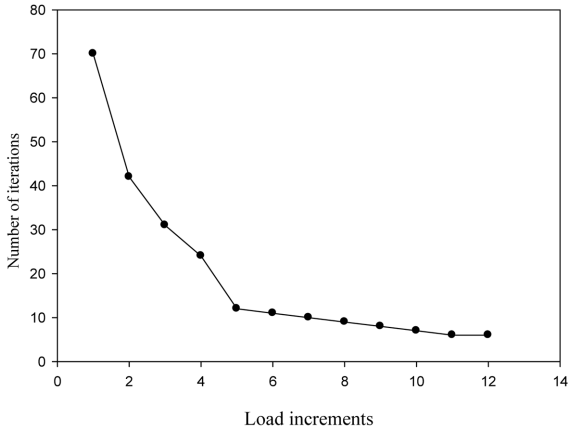

Fig. 4 Plot between load increments and number of iterations

The value of differential settlement between right and middle footings varies from 6.88 mm (first load increment) to 20.87 mm (twelfth load increment) of NLIA. The value of differential settlement provided by LIA is found to be 18.44 mm. The differential settlement between left and middle footings is found to be nearly 14% higher than that between right and middle footings due to NLIA whereas it is nearly 8% due to LIA.

Fig. 4 shows a plot between load increments of NLIA and number of iterations required for each load increments for convergence. It is found that the initially the number of iterations for convergence for first four load increments are more as compared to the remaining load increments.

7.2.2 Contact pressures below footings

Fig. 5 shows the variation of contact pressure below left footing with various load increments of NLIA in the non-dimensional form. The contact pressure increases with increase in load increments. The maximum contact pressure is found below the left edge of the footing whereas it is found to be minimum below the middle of the footing.

The comparison of contact pressures below the left footing provided due to LIA and NLIA at load factor 1.0 (twelfth load increment) reveals that contact pressure at the middle of the footing is almost same due to both analyses but it is found to be nearly 20% more on the left edge of the footing and nearly 9% less on the right edge of the footing due to NLIA.

Fig. 6 shows the variation of contact pressure below middle footing with various load increments of NLIA in the non-dimensional form. The contact pressures distribution is found to be symmetrical with respect to the centre line of the footing. Almost same value of contact pressure exists below the left and right edge of the footing. The contact pressure below the left edge of middle footing is found to be significantly less (nearly 57%) compared to the left edge of left footing. The contact pressure at the left and right edges is nearly 15% more compared to the contact pressure at the

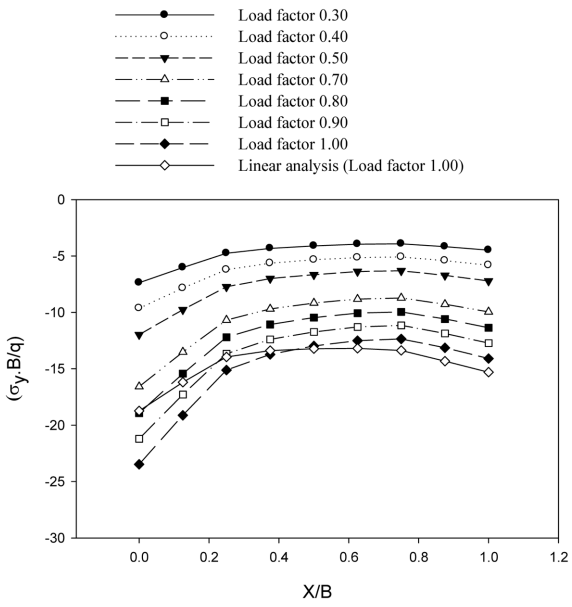

Fig. 5 Variation of contact pressure below left footing of plane frame- layered soil system

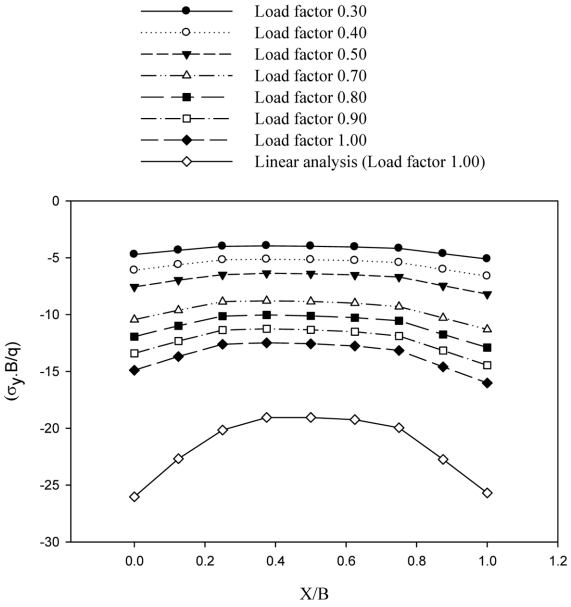

Fig. 6 Variation of contact pressure below middle footing of plane frame- layered soil system

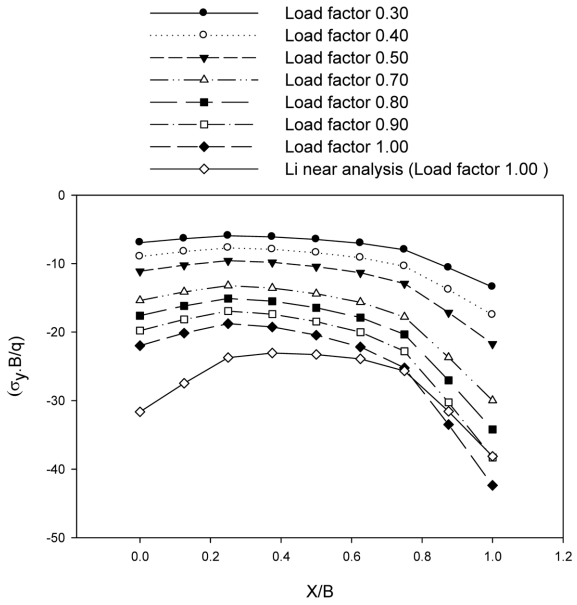

Fig. 7 Variation of contact pressure below right footing for plane frame-layered soil system

middle of the footing. LIA provides significantly higher (nearly 74%) contact pressure compared to NLIA at the left edge of the footing and nearly 60% higher at the right edge of the footing.

Fig. 7 shows the variation of contact pressure below right footing for various load increments of NLIA in the non-dimensional form. The contract pressure at the left edge of the right footing is found to be nearly 92% less compared to the contact pressure at the right edge. The comparison of contact pressure distribution between left and right footing reveals that the contact pressure at the right edge of the right footing is significantly higher nearly by 67%, whereas a marginal decrease of nearly 7% is found at the left edge of the right footing. The increase of nearly 37% is found at the middle of the right footing. LIA provides significantly higher (nearly 30%) contact pressures at the left edge of the footing compared to NLIA whereas it is nearly 11% less at the right edge of the footing.

7.2.3 Axial force in the columns

Table 6 shows the value of axial force in left columns of plane frame-layered soil system due to various analyses. The conventional frame analysis (CFA) is carried out considering the column fixed at their bases. The comparison of axial forces due to CFA and LIA reveals that the interaction effect causes redistribution of the forces in the column members. The inner columns are relieved of the forces and corresponding increase is found in the outer columns due to differential settlements of soil mass.

The interaction effect causes significant increase in the axial forces. A significant increase of nearly 20% to 61% is found in the left columns due to LIA. The maximum increase of nearly 61% is found in the first storey column whereas minimum increase of nearly 20% is found in the top storey column. The comparison of LIA and NLIA reveals that NLIA provides nearly 18 to 43% higher values of axial force in the left columns. Fig. 8 shows the variation of axial force with the load increments of NLIA. The axial force increase with increase in load increments and bilinear

Table 6 Axial force (kN) in left columns of plane frame-layered soil system

Load Factor	Storey Level	Member	CFA	LIA	% Diff. (4 - 5)	NLIA	% Diff. (5 - 7)
1	2	3	4	5	6	7	8
	X	C_1	76.02	91.19	19.95	109.11	19.65
	IX	C_2	145.55	179.98	23.65	212.38	18.00
	VIII	C_3	201.75	256.81	27.29	319.12	24.26
	VII	C_4	248.47	325.55	31.02	407.01	25.02
	VI	C_5	286.72	387.70	35.21	491.97	26.89
1.0	V	C_6	319.34	446.07	39.68	602.93	35.16
	IV	C_7	347.44	501.32	44.28	677.61	35.16
	III	C_8	373.21	556.75	49.17	753.67	35.36
	II	C_9	398.76	616.30	54.55	860.39	39.60
	I	C_{10}	427.88	688.69	60.95	984.95	43.01
	Below GL	C_{11}	497.53	777.68	56.30	1103.32	41.87

Table 7 Axial force (kN) in middle columns of plane frame-layered soil system

Load Factor	Storey Level	Member	CFA	LIA	% Diff. (4 - 5)	NLIA	% Diff. (5 - 7)
1	2	3	4	5	6	7	8
	X	C_{12}	192.66	162.26	-15.77	137.16	-15.46
	IX	C_{13}	372.36	302.70	-18.70	237.09	-21.67
	VIII	C_{14}	550.05	438.69	-20.24	344.41	-21.49
	VII	C_{15}	725.90	569.56	-21.53	415.90	-26.97
	VI	C_{16}	900.96	696.63	-22.67	493.66	-29.13
1.0	V	C_{17}	1075.92	819.58	-23.82	561.92	-31.43
	IV	C_{18}	1251.62	941.38	-24.78	639.82	-32.03
	III	C_{19}	1428.31	1059.10	-25.84	689.18	-34.92
	II	C_{20}	1606.62	1175.56	-26.83	742.24	-36.86
	I	C_{21}	1785.64	1289.14	-27.80	801.50	-37.82
	Below GL	C_{22}	1951.74	1263.16	-35.28	808.80	-35.97

variation is found. The maximum axial force is found in the column below ground level.

Table 7 shows the value of axial force in middle columns of plane frame-layered soil system due to various analyses. LIA reveals that the interaction effect causes decrease in the axial force in the middle columns due to differential settlements. A significant decrease of nearly 15% to 35% is found in the middle columns due to LIA. The maximum decrease of nearly 35% is found in the column below ground level whereas minimum decrease of nearly 15% is found in the top storey column. The comparison of LIA and NLIA reveals that NLIA provides nearly 15 to 38% lower values of axial force in the middle columns. Fig. 9 shows the variation of axial force with the load increments of NLIA. The axial force in the columns varies in bilinear manner. The maximum axial force is found in the column below ground level.

Table 8 shows the value of axial force in right columns of plane frame-layered soil system due to various analyses. The interaction effect causes significant increase in the axial force in the right columns due to LIA. A significant increase of nearly 9% to 17% is found in the right columns. The axial force in the right columns increases nearly by 17% except in the column below ground level,

Table 8 Axial force (kN) in right columns of plane frame-layered soil system

Load Factor	Storey Level	Member	CFA	LIA	% Diff. (4 - 5)	NLIA	% Diff. (5 - 7)
1	2	3	4	5	6	7	8
1.0	X	C_{23}	91.34	106.67	16.78	129.71	21.59
	IX	C_{24}	202.09	236.71	17.13	270.92	14.45
	VIII	C_{25}	328.16	383.53	16.87	441.71	15.16
	VII	C_{26}	465.54	543.17	16.67	626.21	15.28
	VI	C_{27}	612.24	714.79	16.74	827.97	15.83
	V	C_{28}	764.64	893.30	16.82	1015.81	13.71
	IV	C_{29}	920.85	1077.47	17.00	1241.32	15.20
	III	C_{30}	1078.36	1263.03	17.12	1451.88	14.95
	II	C_{31}	1234.49	1446.41	17.16	1675.64	15.84
	I	C_{32}	1386.36	1623.95	17.13	1861.90	14.65
	Below GL	C_{33}	1567.24	1716.45	9.52	1857.16	8.19

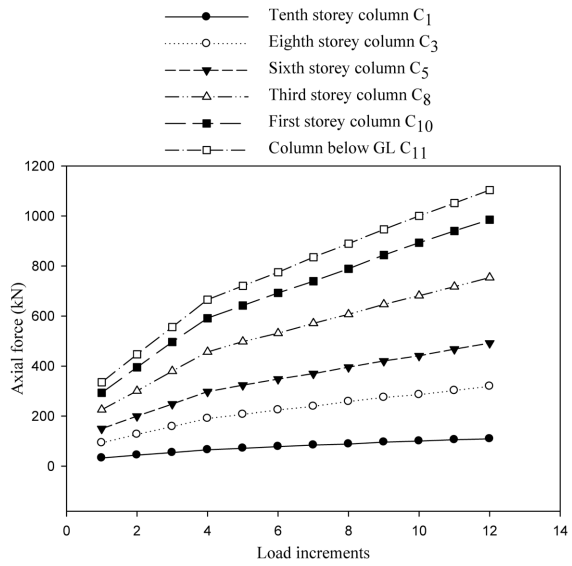

Fig. 8 Variation of axial force in left columns of plane framelayered soil system for nonlinear analysis

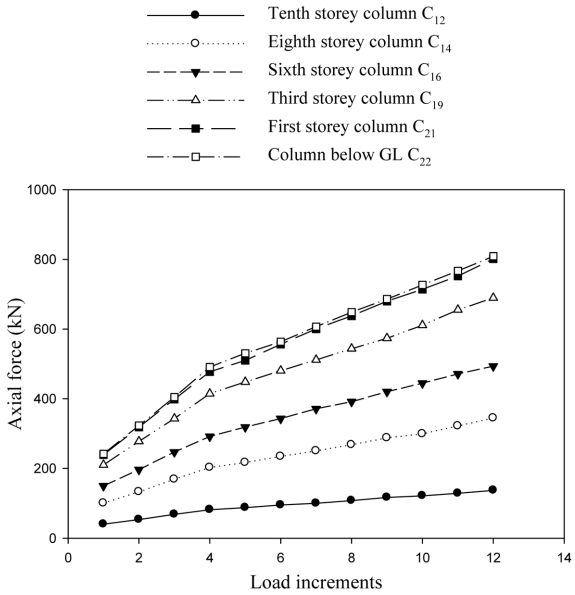

Fig. 9 Variation of axial force in middle columns of plane framelayered soil system for nonlinear analysis

where increase of nearly 9% is found. The comparison of LIA and NLIA reveals that NLIA provides nearly 8 to 21% higher values of axial force in the right columns. The increase in axial force due to interaction effect in the left columns is significantly higher than that found in the right columns. Fig. 9 shows the variation of axial force in right columns with the load increments of NLIA. The bilinear variation in axial force is found. The maximum axial force is found in the first storey column.

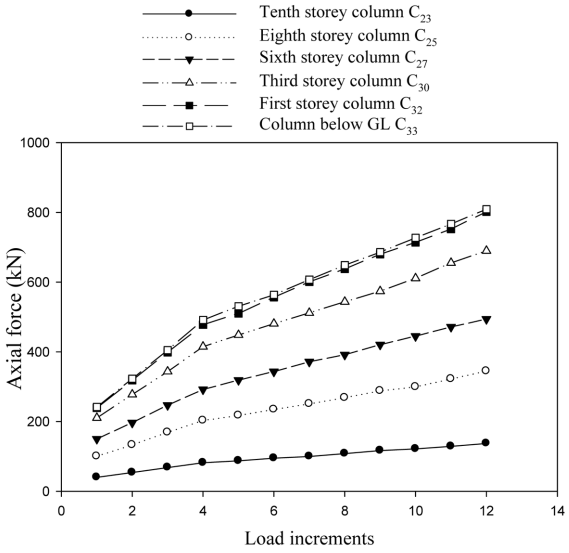

Fig. 10 Variation of axial force in right columns of plane framelayered soil system for nonlinear analysis

Table 9 Bending moments (kN-m) in left columns of plane frame-layered soil system

Load Factor	Storey Level	Member	NIA	LIA	% Diff. (4 - 5)	NLIA	% Diff. (5 - 7)
1	2	3	4	5	6	7	8
1.0	X	C_1	-23.03	-48.62	111.11	-74.59	53.42
			-22.73	-44.27	94.76	-65.88	48.81
	IX	C_2	9.18	-7.98	*	-26.30	229.57
			3.61	-12.72	*	-29.89	134.98
	VIII	C_3	12.09	-14.24	*	-41.45	191.08
			5.83	-18.87	*	-44.29	134.71
	VII	C_4	30.16	8.02	-73.40	-15.50	*
			25.14	4.37	-82.62	-17.32	*
	VI	C_5	28.99	-1.48	*	-33.13	**
			24.46	-4.23	*	-34.46	**
	V	C_6	41.61	15.07	-63.78	-13.41	*
			39.38	14.61	-62.90	-12.11	*
	IV	C_7	36.09	0.90	-97.50	-36.05	*
			36.68	5.23	-85.74	-28.13	*
	III	C_8	43.63	9.56	-78.08	-27.05	*
			53.08	26.47	-50.13	-2.35	*
	II	C_9	26.43	-22.58	*	-74.47	229.80
			51.03	27.07	-46.95	8.54	-68.45
	I	C_{10}	19.53	-49.14	*	-132.59	169.82
			69.16	124.57	-80.12	88.62	-28.85
	Below GL	C_{11}	-13.53	-220.98	**	-338.12	53.01
			130.55	-194.55	*	-390.63	100.78

*reversal in sign, **Very high difference in values

7.2.4 Bending moments in the columns

Table 9 shows the values of bending moment in the left columns of plane frame-layered soil system. The interaction effect causes significant variation in bending moments of left and right columns. This is because of the transfer of moments from the interior columns to the outer columns due to differential settlements. A decrease of nearly 47% to 97% is found in the bending moments of left columns due to LIA. The maximum decrease in the bending moment is found to be nearly 97% in the column of fourth storey whereas maximum increase of nearly 111% is found at the roof level of the top storey column. The reversal in the sign of bending moments is found in the columns of 6th, 8th and 9th storeys. A significant increase in the bending moment of column below ground level is found. The comparison between LIA and NLIA shows that NLIA provides variation of nearly 53% to 230% higher than that provided by LIA. Fig. 11 shows variation of bending moments in the left columns due to NLIA. The bending moments increase with increase in load increments and bilinear variation is found.

Table 10 shows the values of bending moment in the middle columns of plane frame-layered soil system. The interaction effect causes almost insignificant variation in bending moments of all the

Table 10 Bending moments (kN-m) in middle columns of plane frame-layered soil system

Load Factor	Storey Level	Member	NIA	LIA	% Diff. (4 - 5)	NLIA	% Diff. (5 - 7)
1	2	3	4	5	6	7	8
1.0	X	C_{12}	34.01 22.64	34.07 22.66	0.17 0.08	34.00 22.17	-0.20 -2.16
	IX	C_{13}	69.33 57.26	69.61 57.46	0.40 0.35	68.92 57.18	-0.99 -0.48
	VIII	C_{14}	98.11 83.17	98.50 83.41	0.39 0.28	96.97 83.42	-1.55 -0.01
	VII	C_{15}	118.43 106.02	119.08 106.55	0.54 0.49	117.55 104.79	-1.28 -1.65
	VI	C_{16}	135.24 123.20	136.03 123.97	0.58 0.62	134.17 122.25	-1.36 -1.38
	V	C_{17}	143.41 134.99	144.06 136.12	0.45 0.84	141.25 134.02	-1.95 -1.54
	IV	C_{18}	150.64 147.49	150.14 149.26	-0.33 1.20	145.67 148.14	-2.97 -0.75
	III	C_{19}	146.14 148.10	142.05 155.08	-2.80 4.71	133.56 157.58	-5.97 1.61
	II	C_{20}	144.65 176.28	122.67 195.73	-15.19 11.03	97.11 226.88	-20.83 15.91
	I	C_{21}	100.17 212.84	39.71 318.83	-60.35 49.80	-44.85 348.90	* 9.43
	Below GL	C_{22}	12.23 287.15	-220.75 -63.47	* *	-394.62 -8.81	78.76 -86.12

*reversal in sign

columns except the columns of first storey where decrease of nearly 60% is found in the bending moment at the top of the column whereas increase of nearly 50% is found at the bottom end of the column due to LIA. The reversal in the sign of bending moment is found in the column below ground level. NLIA also provides insignificant variation in the bending moments of all columns except the column below ground level where increase of nearly 79% is found at the top of the column and decrease of nearly 86% is found at the bottom of the column. A reversal in the sign of bending moment is found in the bending moment at the top of the column of first storey. Fig. 12 shows variation of bending moments in the middle columns due to NLIA. The bilinear variation in the bending moments is found.

Table 11 shows the values of bending moment in the right columns of plane frame-layered soil system. An increase of nearly 24% to 48% is found in the bending moments of all the columns except the column of first storey where decrease of nearly 19% is found at the bottom due to LIA. The maximum increase of nearly 230% is found in the column below ground level. NLIA provides variation of nearly 18% to 33% compared to LIA. The reversal in the sign of bending moment is found at the top of column below ground level.

Table 11 Bending moments (kN-m) in right columns of plane frame-layered soil system

Load Factor	Storey Level	Member	NIA	LIA	% Diff. (4 - 5)	NLIA	% Diff. (5 - 7)
1	2	3	4	5	6	7	8
1.0	X	C_{23}	57.93 44.94	83.63 66.55	44.36 48.08	109.02 88.43	30.36 32.87
	IX	C_{24}	62.14 53.31	79.61 69.87	28.11 31.06	96.88 86.41	21.69 23.67
	VIII	C_{25}	90.08 77.69	116.79 102.72	29.65 32.21	143.28 127.31	22.68 23.93
	VII	C_{26}	92.78 82.70	115.57 104.07	24.56 25.84	137.03 124.62	18.56 19.74
	VI	C_{27}	109.91 98.96	141.76 128.46	28.97 29.81	171.59 156.76	21.04 22.03
	V	C_{28}	107.32 99.87	134.50 125.84	25.32 26.00	160.06 150.58	19.00 19.65
	IV	C_{29}	115.56 109.86	150.26 144.46	30.02 31.49	183.49 177.65	22.11 22.97
	III	C_{30}	109.06 113.39	137.57 146.88	26.14 29.53	164.73 180.64	19.74 22.98
	II	C_{31}	101.93 120.81	129.60 172.88	27.14 43.10	152..70 203.18	17.82 17.52
	I	C_{32}	84.52 136.97	82.64 110.95	-2.22 -18.99	103.76 252.39	25.55 127.48
	Below GL	C_{33}	30.30 147.69	100.00 250.00	230.03 69.27	-36.82 725.50	* 190.22

*reversal in sign

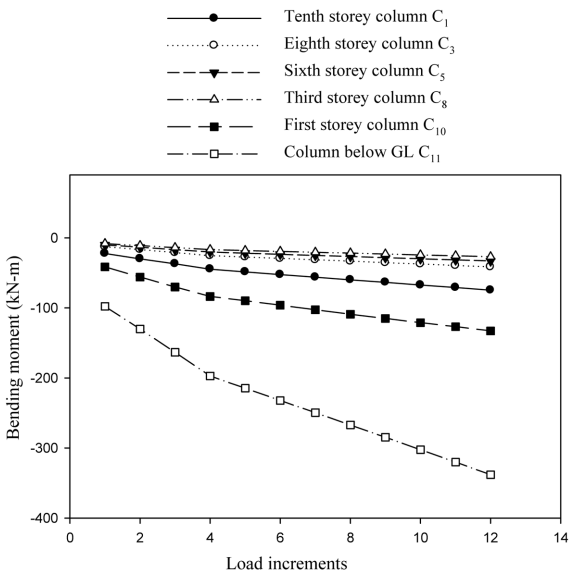

Fig. 11 Variation of bending moment at roof level in left columns of plane frame-layered soil system for nonlinear analysis

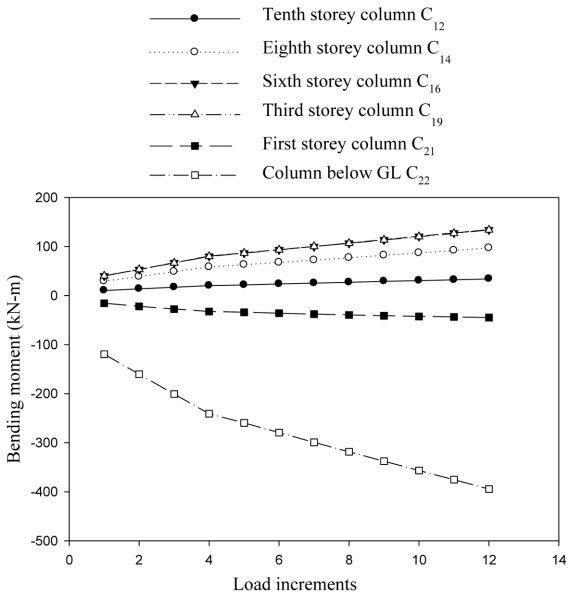

Fig. 12 Variation of bending moment at roof level in middle columns of plane frame-layered soil system for nonlinear analysis

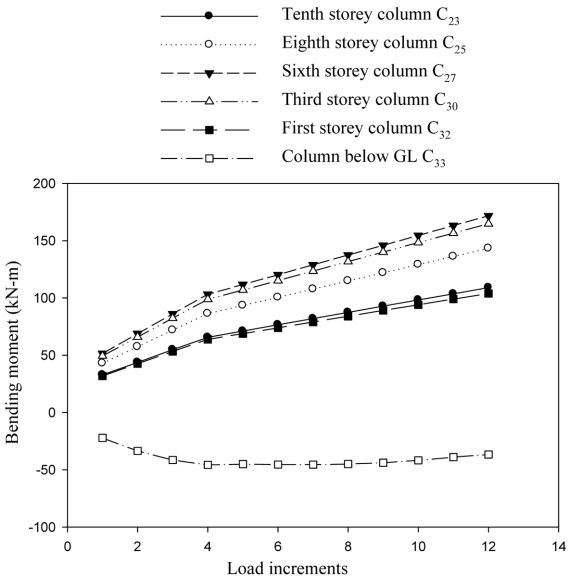

Fig. 13 Variation of bending moment at roof level in right columns of plane frame-layered soil system for nonlinear analysis

Fig. 13 shows variation of bending moments in the right columns due to NLIA. The bilinear variation in the bending moments is found.

7.2.5 Bending moments in the floor beams

7.2.5.1 Bending moment in floor beams of left bay

Table 12 shows the values of bending moment at the left and right ends of the floor beams of left bay of plane frame-layered soil system. The interaction effect causes transfer of bending moments from the right end to the left end of in all floor beams due to differential settlements between left and middle column footings. The significant decrease of nearly 81 to 95% is found in the bending moment at the left end of the floor beams. The minimum decrease of nearly 81% is found in the floor beam of third storey and maximum decrease of nearly 95% is found in the floor beam of second storey. The significant increase of nearly 111% is found in the floor beam of tenth storey whereas a highly significant increase of nearly 285% is found in the floor beam of second storey. The reversal in the sign of bending moment is found at the left end of first, seventh and eighth storeys as well as in the plinth beam.

A decrease of nearly 31 to 48% is found at the right end of all the floor beams except in the plinth beam where reversal in the sign of bending moment is found. The minimum decrease of

Table 12 Bending moments (kN-m) in floor beam of left bay of plane frame-layered soil system

Load Factor	Storey Level	Member	NIA	LIA	% Diff. (4 - 5)	NLIA	% Diff. (5 - 7)
1	2	3	4	5	6	7	8
1.0	X	B_1	23.04 -85.98	48.63 -44.25	111.06 -48.53	74.30 -2.23	52.78 -94.96
	IX	B_3	13.54 -105.64	52.25 -57.22	285.89 -45.83	91.89 -7.85	75.86 -86.28
	VIII	B_5	-15.70 -136.38	26.95 -85.41	* -37.37	72.32 -33.63	168.34 -60.62
	VII	B_7	-36.00 -158.74	10.86 -104.96	* -33.87	59.64 -49.49	449.17 -52.84
	VI	B_9	-54.13 -178.72	-2.90 -121.73	-94.64 -31.88	51.19 -61.12	* -49.79
	V	B_{11}	-66.07 -192.13	-10.84 -132.04	-83.59 -31.27	46.00 -68.17	* -48.37
	IV	B_{13}	-75.47 -203.06	-15.51 -138.97	-79.44 -31.56	48.81 -69.46	* -50.02
	III	B_{15}	-80.32 -208.73	-14.80 -139.79	-81.57 -33.02	54.32 -65.89	* -52.86
	II	B_{17}	-79.52 -210.48	-3.88 -131.49	-95.12 -37.52	76.15 -47.94	* -63.54
	I	B_{19}	-70.55 -203.43	22.07 -108.50	* -46.66	124.34 -3.95	463.39 -96.36
	Plinth level	PB_1	-55.63 -170.61	96.39 15.47	* *	249.34 125.66	158.67 712.28

*reversal in sign

nearly 31% is found in the floor beam of fifth storey whereas the maximum decrease of nearly 48% is found in the floor beam of tenth storey.

The comparison between LIA and NLIA reveals that NLIA provides significant variation in bending moments at both the ends of all floor beams. The significant increase of nearly 52 to 463% is found in the bending moment at the left end of floor beams except in the floor beams of second to sixth storeys where reversal in the sign of bending moment is found. A significant decrease of nearly 50 to 96% is found in the bending moment at the right end of floor beam due to NLIA as compared to LIA. A very high increase in bending moment is found in the plinth beam.

7.2.5.2 Bending moment in floor beams of right bay

Table 13 shows the values of bending moment at the left and right ends of the floor beams of right bay of plane frame-layered soil system. The interaction effect causes transfer of bending moments from the right end to the left end of in all floor beams due to differential settlements

Table 13 Bending moments (kN-m) in floor beam of right bay of plane frame-layered soil system

Load Factor	Storey Level	Member	NIA	LIA	% Diff. (4 - 5)	NLIA	% Diff. (5 - 7)
1	2	3	4	5	6	7	8
1.0	X	B_2	51.97 -57.92	10.18 -83.63	-80.41 44.38	-32.45 -108.53	* 29.77
	IX	B_4	13.67 -107.08	-35.08 -146.15	* 36.48	-85.08 -185.63	142.53 27.01
	VIII	B_6	-18.99 -143.38	-70.52 -186.65	271.35 30.18	-121.53 -229.81	72.33 23.12
	VII	B_8	-42.88 -170.46	-97.54 -218.26	127.47 28.08	-152.20 -264.15	56.03 21.02
	VI	B_{10}	-62.54 -192.60	-120.83 -245.22	93.20 27.32	-178.61 -296.24	47.82 20.80
	V	B_{12}	-74.49 -206.27	-135.99 -262.98	82.56 27.49	-195.49 -318.32	43.75 21.04
	IV	B_{14}	-82.57 -215.43	-147.27 -276.10	78.35 28.16	-209.99 -333.33	42.59 20.73
	III	B_{16}	-84.91 -218.92	-151.54 -282.03	78.47 28.82	-214.49 -341.63	41.54 21.12
	II	B_{18}	-82.27 -215.32	-146.28 -276.49	77.80 28.40	-205.87 -333.09	40.74 20.47
	I	B_{20}	-73.02 -205.32	-126.93 -255.53	73.83 24.45	-177.27 -307.45	39.65 20.31
	Plinth level	PB_2	-54.46 -167.27	-113.55 -210.97	108.50 26.12	-80.37 -215.83	- 29.22 2.30

*reversal in sign

between right and middle column footings. The significant increase of nearly 73 to 271% is found in the bending moment at the left end of the floor beams of right bay. The minimum increase of nearly 73% is found in the floor beam of first storey and maximum increase of nearly 271% is found in the floor beam of eighth storey. The significant decrease of nearly 80% is found in the floor beam of tenth storey whereas an increase of nearly 108% is found in the plinth beam. The reversal in the sign of bending moment is found at the left end of ninth storey.

The significant increase of nearly 24 to 44% is found at the right end of all the floor beams including plinth beam. The minimum increase of nearly 24% is found in the floor beam of first storey whereas the maximum increase of nearly 44% is found in the floor beam of tenth storey.

The comparison between LIA and NLIA reveals that NLIA provides significantly higher values of bending moments at both the ends of all floor beams. The significant increase of nearly 39 to 142% is found in the bending moment at the left end of all floor beams except in the plinth beam where decrease in bending moment of nearly 29% is found. The reversal in the sign of bending moment is found at the left end of the floor beam of tenth storey. A significant increase of nearly 20 to 30% is found in the bending moment at the right end of floor beam due to NLIA as compared to LIA. An insignificant increase in bending moment at the right end of the plinth beam is found.

Fig. 14 and Fig. 15 shows the variation of bending moments in the floor beams with differential settlements due to nonlinear interaction analysis. The bending moments in the floor beams increase with the increase in differential settlements. The bilinear variation in bending moment in is found.

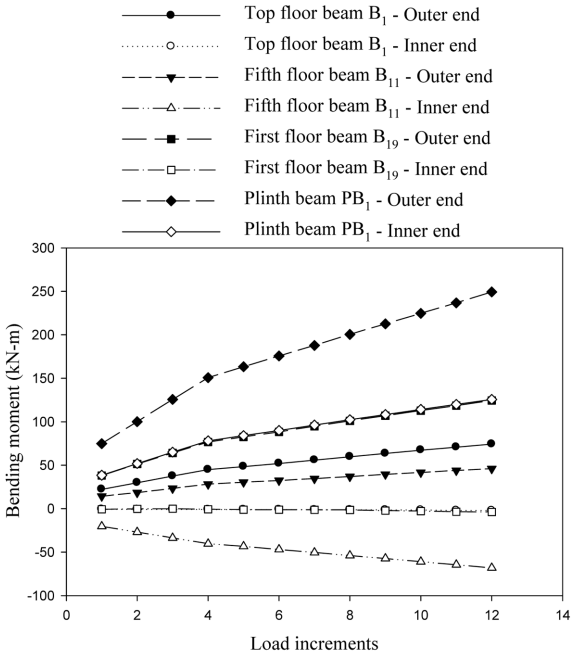

Fig. 14 Variation of bending moments in floor beams of left bay of plane frame-layered soil system for nonlinear analysis

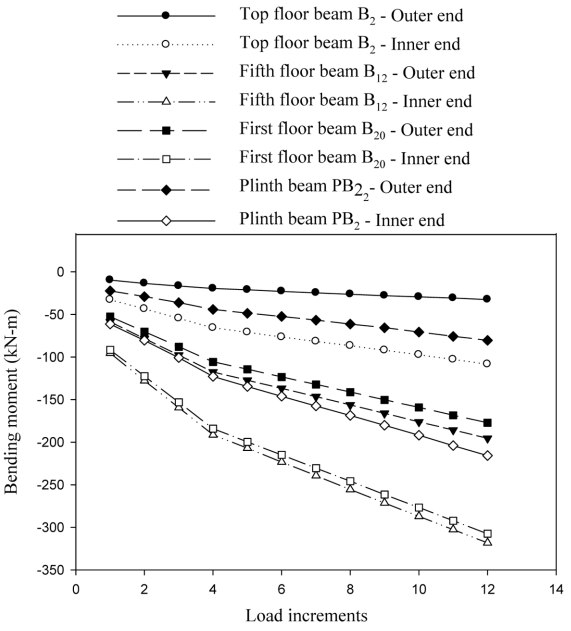

Fig. 15 Variation of bending moments in floor beams of right bay of plane frame-layered soil system for nonlinear analysis

8. Conclusions

(i) The forces in the various frame members due to interaction analysis are considerably different from the conventional frame analysis.
(ii) The differential settlement causes significant redistribution in the forces in frame members. The differential settlement between left and middle footings is significantly higher than that between right and middle footings. The nonlinear analysis suggests that differential settlements as well as forces in the frame members vary in bilinear manner.
(iii) The middle columns are relieved of the axial forces and corresponding increase in axial force is found in the left and right columns due to differential settlements of soil mass.
(iv) The interaction effect causes transfer of bending moments from the right end to the left end in all floor beams due to differential settlements and there is highly significant increase in the bending moments.
(v) The contact pressures below the right column footing are significantly higher as compared to the left and middle column footings.
(vi) The interaction effect causes transfer of bending moments from the interior columns to the exterior columns due to differential settlements. A significant decrease in bending moments is found in the left columns whereas significant increase is found in the right columns. The reversal in the sign of bending moments is found in floor beams of upper storeys. The nonlinear analysis provides significantly higher values of forces in the frame members.

References

Aljanabi, A.I.M., Farid, B.J.M. and Mohamad, A.A.A. (1990), "Interaction of plane frames with elastic foundation having normal and shear moduli of subgrade reactions", *Int. J. Comput. Struct.*, **36**(6), 1047-1056.
Allam, M.M., Rao, S. and Subramanyam, K.S. (1991), "Frame soil interaction and Wrinkler model", *Proceedings of Institution of Civil Engineers*, Part 2, 477-494.
Abate, G., Massimino, M.R. and Maugeri, M. (2007), "Soil plasticity and uplifting effects on soil-structure interaction", Workshop of ETC-12 Evaluation Committee for the Application.
Asteris, P.G. (2008), "Finite element micro modeling of infilled frames", *Electr. J. Struct. Eng.*, **8**, 1-11.
Asteris, P.G. (2003), "Lateral stiffness of brick masonry infilled plane frames", *J. Struct. Eng.*, **129**(8), 1071-1079.
Baker, A.L.L. (1957), *Raft Foundations, Concrete Publications Limited*, London.
Brown, P.T. and Yu, K.R. (1986), "Load sequence and structure-foundation-interaction", *J. Struct. Div.-ASCE*, **112**(3), 481-488.
Chameski, C. (1956), "Structural rigidity in calculating settlements", *J. Soil Mech. Found. Div.*, **82**(SM1), 477-494.
Duncan, J.M. and Chang, C.Y. (1970), "Nonlinear analysis of stress and strain in soils", *J. SM FE, ASCE*, **96**, 1629-1654.
Dutta, S.C., Maity, A. and Moria, D. (1999), "Effect of soil-structure interaction on column moment of building frames", *J. Inst. Engineers, Indian*, **80**, 1-7.
Francis, A.J. (1953), "Some recent developments in structural analysis and design", *Proceedings of Engg. Conf. Melbourne, Inst. Eng.*, Australia.
Fardis, M.N. and Panagiotakos, T.B. (1997), "Seismic design and response of bare and masonry-infilled reinforced concrete buildings part II: Infilled structures", *J. Earthq. Eng.* **1**(3), 475-503.
Grashoff, H. (1957), "Influence of flexural rigidity of superstructure on the distribution of contact pressure and bending moment of an elastic combined footing", *Proceedings of 4th Int. Conf. SM & FE, London*, **1**, 300-

306.
Hinton, E. and Owen, D.R.J. (1977), *Finite Element Programming*, Academic Press, London.
Hora, M. and Patel, A.N. (2005), "Computational Methodology for non-linear soil-structure interaction analysis of infilled building frames", *Proceeding of Int. Geot. Conf. St. Petersburg*, **1**, 175-181.
Hora, M. (2006), "Nonlinear interaction analysis of infilled building frame-soil system", *J. Struct. Eng.*, **33**(4), 309-318.
Jain, O.P., Trikha, D.N. and Jain, S.C. (1977), "Differential foundation settlement of high rise buildings", *Proceedings of Int. Symp. on Soil- Structure Interaction*, University of Roorkee, Roorkee, India, **1**, 237-244.
Kondner, R.L. and Zelasko, J.S. (1963), "A hyperbolic stress-strain formulation for sands", *Proceedings of Second Pan-American Conf. SM & FE, Brazil*, **1**, 289-324.
Kim, D.K. and Yun, C.B. (2003), "Time domain earthquake response analysis method for 2-D soil-structure interaction systems", *J. Struct. Eng. Mech.*, **15**(6), 717-733.
King, G.J.W. and Chandrasekaran, V.S. (1974), "An assessment of the effects of interaction between a structure and its foundation", *Proceedings of Conf. on Settlement of Structures*, British, Geotechnical, Cambridge.
King, G.J.W. and Yao, Z.E. (1983), "Simplified interactive analysis of long framed buildings on raft foundation", *J. Struct. Eng.,* **16**(3), 62-67.
Kaushik, H.B., Rai, D.C. and Jain, S.K. (2006), "Code approaches to seismic design of masonry-infilled reinforced concrete frames: A state-of-the-art review", *Earthq. Spectra*, **22**, 961-983.
Larnach, W.J. (1970), "Computation of settlement of building frames", CV7 Engineering Publication Works, Revision, **65**, 1040-1044.
Lee, I.K. and Brown, P.T. (1972), "Structure-foundation interaction analysis", *J. Struct. Div.-ASCE*, **98**, ST11, 2413-2431.
Meyerhoff, G.G. (1947), "The settlement analysis of building frames", *Struct. Eng.*, **25**, 53-63.
Morris, D. (1966), "Interaction of continuous frames and soil media", *J. Struct. Div.-ASCE*, **5**, 13-43.
McCallen, D.B. and Romstad, K.M. (1993), "A nonlinear model for building soil systems, Part I: Formulation", Rep. UCRL-JC-112107 part I, Lawrence Livermore, National Laboratory, Livermore, California, USA.
Mandal, A. (1998), "Soil-structure interaction on building frame: a small scale model study", *Int. J. Struct.*, **18**(2), 92-108.
Manos, G.C., Thaumpta, J. and Yasin, B. (2000), "Influence of masonry infills on the earthquake response of multi-storey reinforced concrete structures", *Proceedings of the 12th World Conference on Earthquake Engineering*, Auckland, New Zealand.
Mohebkhah, A., Tasnimi, A.A. and Moghadam, H.A. (2008), "Nonlinear analysis of masonry-infilled steel frames with openings using discrete element method", *J. Constr. Steel Res.*, **64**(12), 1463-1472.
Monica, P., Maylet, U. and Julio, F.L. (2009), "Modeling of masonry of infilled frames, Part I: The plastic concentrator", *Eng. Struct.*, **31**(1), 113-118.
Nayak, G.C. and Zienkiewicz, O.C. (1972), "Elasto-plastic, stress analysis – a generalization for various constitutive relations including strain softening", *Int. J. Numer. Math. Eng*., **5**, 113-135.
Noorzaei, J., Viladkar, M.N. and Godbole, P.N. (1991), "Soil-structure interaction of space frame-raft-soil system – A parametric study", *Int. J. Comput. Struct.*, **36**(6), 1235-1247.
Seetharamulu, K. and Kumar, A. (1973), "Interaction of foundation beams and soil with frames", *Proceedings of 8th Int. Conf. on SM & FE*, Moscow, USSR, 231-234.
Subbarao, K.S., Shardaa Bai, H. and Rangnathan, B.V. (1985), "Interaction analysis of frames with beam footing", *Proceedings of Indian Geotech. Cont., University of Roorkee*, **1**, 389-395.
Selvadurai, A.P.S. and Karpurapu, R. (1989), "Composite infinite element for modelling unbounded saturated soil media", *J. Geotech. Eng.-ASCE*, **1.15**(7), 1633-1646.
Sharda Bai, H., Rao, Subba, K.S. and Rangnathan B.V. (1990), "Interaction behaviour of elasto-plastic plane frames with isolated footings on soil", *Proceedings of Indian Geotech. Conf.*, Bombay.
Viladkar, M.N., Godbole, P.N. and Noorzaei, J. (1991), "Soil-structure interaction in plane frames using coupled finite-infinite elements", *Int. J. Comput. Struct.*, **39**(5), 535-546.
Viladkar, M.N., Godbole, P.N. and Noorzaei, J. (1994), " Nonlinear soil-structure interaction in plane frames", *Int. J. Comput. Struct.*, **11**, 303-316.